NeuroImage 49 (2010) 1612–1621

Contents lists available at ScienceDirect

NeuroImage

journal homepage: www.elsevier.com/locate/ynimg

A multimodal brain imaging study of repetition suppression in the human visual cortex

Rishma Vidyasagar [a,*], Andrej Stancak [b], Laura M. Parkes [a,c]

[a] MARIARC, University of Liverpool, Pembroke Place, Liverpool L69 3GE, UK
[b] School of Psychology, University of Liverpool, The Eleanor Rathbone Building, Bedford Street South, Liverpool L69 7ZA, UK
[c] Imaging Science and Biomedical Engineering, School of Cancer and Imaging Sciences, University of Manchester, Stopford Building, Oxford Rd, M13 9PT, UK

ARTICLE INFO

Article history:
Received 14 May 2009
Revised 7 October 2009
Accepted 7 October 2009
Available online 23 October 2009

Keywords:
Repetition Suppression
Visual Cortex
MEG
fMRI
Behaviour
Adaptation

ABSTRACT

Repetition suppression (RS) relates to a reduced neuronal response to a stimulus that is repeated. This phenomenon has been observed in the visual ventral stream and other sensory modalities, suggesting that it is a common feature of neuronal processing. Whilst a number of different models have been suggested to explain the underlying neural mechanisms of RS, they are difficult to test due to variety in paradigm design and the limited resolution of different measuring modalities. This study combined information from different modalities using the same paradigm across the same subjects, in an attempt to create a clearer link between fMRI, magnetoencephalography (MEG) and behaviour data, and thus better understand the underlying mechanism of neuronal RS. We used an oriented Gabor patch stimulus separated by two possible interstimulus intervals of 200 or 600 ms and two possible orientation combinations: the second patch was consistently vertical combined with the first patch which was either horizontal (DIFF) or vertical (SAME). For the 200 -ms condition only, behavioural data showed a statistically significant impairment in subjects' ability to discern the direction of tilt at the SAME condition compared to the DIFF condition; fMRI showed suppression of the BOLD response, and MEG showed suppression of the peak amplitude. A significant correlation between the suppressed BOLD and MEG signals confirm the neuronal origin of the BOLD suppression effect. Measurements from the 3 modalities suggest that neuronal RS in the visual cortex in the current orientation-driven paradigm can be best explained by an overall reduction in the size of the response of all neurons (fatigue model) or a reduction in the number of neurons responding (sharpening model).

Introduction

Repetition suppression (RS) is a phenomenon that refers to a reduction in the response to a repeated stimulus as measured by single-cell recordings in animals (Movshon and Lennie, 1979; Sawamura et al., 2006) or functional magnetic resonance imaging (fMRI) in humans(Grill-Spector et al., 1999; Henson and Rugg, 2003; Murray et al., 2006). Neuronal RS occurs in neurons that are tuned to particular stimulus characteristics that are repeated. It is this feature that is believed to be reflected by fMRI RS measurements utilising fMRI blood oxygen level dependent (BOLD) signal. fMRI RS studies are also referred to as fMR-adaptation and have been used to study specific systems such as the ventral stream of the visual system (Grill-Spector et al., 1999; Kourtzi and Kanwisher, 2001; Sawamura et al., 2005; Vuilleumier et al., 2002). In these studies, fMRI RS was used as a tool to gain sub-voxel information from cortical regions that code for different aspects of a visual stimulus such as contour and shape. Whilst fMR-adaptation paradigms are incorporated in many fMRI studies, to date, there has yet to be a clear relation between RS observed in fMRI-BOLD signal changes and corresponding neuronal responses. This link could help clarify the underlying neuronal mechanisms of fMRI-RS and aid in accurate interpretation of fMR-adaptation studies. Whilst the BOLD signal yields a sensitive indicator of regional cerebral activity and provides good spatial resolution, it is not a direct measure of neural activity and has poor temporal resolution (s). Magnetoencephalography (MEG), however has the advantage of measuring magnetic flux derived from the electrical activity of neurons, thus is a comparatively direct measure of neuronal activity, and provides good temporal resolution (ms), with the drawback of limited spatial resolution compared to that of fMRI.

Conflicting neuronal models of RS arise for many reasons, such as limitations of single modality measurements that may be sensitive to only specific information, i.e. temporal or spatial information (Murray and Wojciulik, 2004); diversity in paradigm designs such as stimulus timing; and the objectives of certain paradigms, for example using faces as stimuli which will require higher level processing. It is possible that different paradigms produce RS caused by different underlying mechanisms. Three possible mechanisms suggested by

* Corresponding author.
E-mail address: rishmav@liv.ac.uk (R. Vidyasagar).

1053-8119/$ – see front matter © 2009 Elsevier Inc. All rights reserved.
doi:10.1016/j.neuroimage.2009.10.020

Grill-Spector et al. (2006) are the fatigue, sharpening and facilitation models. These models were proposed to explain underlying neuronal behaviour with regards to fMRI-RS signal. The fatigue model (Fig. 1B) proposes an overall reduction in firing rate from all responsive neurons in the population, whilst the "sharpening" model (Fig. 1C) suggests a reduction in the number of neurons that respond to the repeated stimulus. This model predicts a response from neurons that are highly tuned to the stimulus characteristics that are repeated, and an inhibition of the more weakly tuned neurons. The final model referred to as the "facilitation model" (Fig. 1D) proposes an effect on the temporal processing of the repeated stimuli, i.e. a reduction in processing time and therefore quicker neuronal response upon the presentation of the repeated (Becker et al., 1997; Henson, 2003; James and Gauthier, 2006). Potentially, all three models may be relevant in different cortical regions, or under different paradigm conditions.

The aim of this study was to observe the response to an identical stimulus paradigm using three measurement modalities: fMRI, MEG and behavioural measurements. Studying the same paradigm using the two modalities in conjunction with behavioural measurements, we hoped to discern a clearer understanding of the role of the three models in RS. A behavioural component was incorporated into the study for two reasons. Past studies have shown that attention improves the firing of neurons to a task, however, Murray and Wojciulik (2004) have shown that an attention component can also enhance fMRI-RS. The behavioural task was also included to potentially aid in the interpretation and understanding of the consequence of neuronal-RS.

The visual cortex was chosen as it is relatively well characterised for its coding of specific stimulus features (Slotnick and Yantis, 2003). We chose to look at orientation coding in the visual cortex as the spatial organisation of columns of neurons tuned to different orientations in V1 is well documented (Bonhoeffer and Grinvald, 1991; Hubel and Wiesel, 1968). We analysed the fMRI data from all visual areas activated (not only V1 and V2), to determine whether RS is also present in areas thought not to be orientation-selective. The paradigm used in all 3 measurement modalities incorporated paired Gabor patches of SAME (vertical–vertical) and DIFF (horizontal–vertical) orientations. Observation of RS was expected for the SAME condition relative to the DIFF condition, as for the DIFF condition different neuronal populations will be activated for each Gabor patch

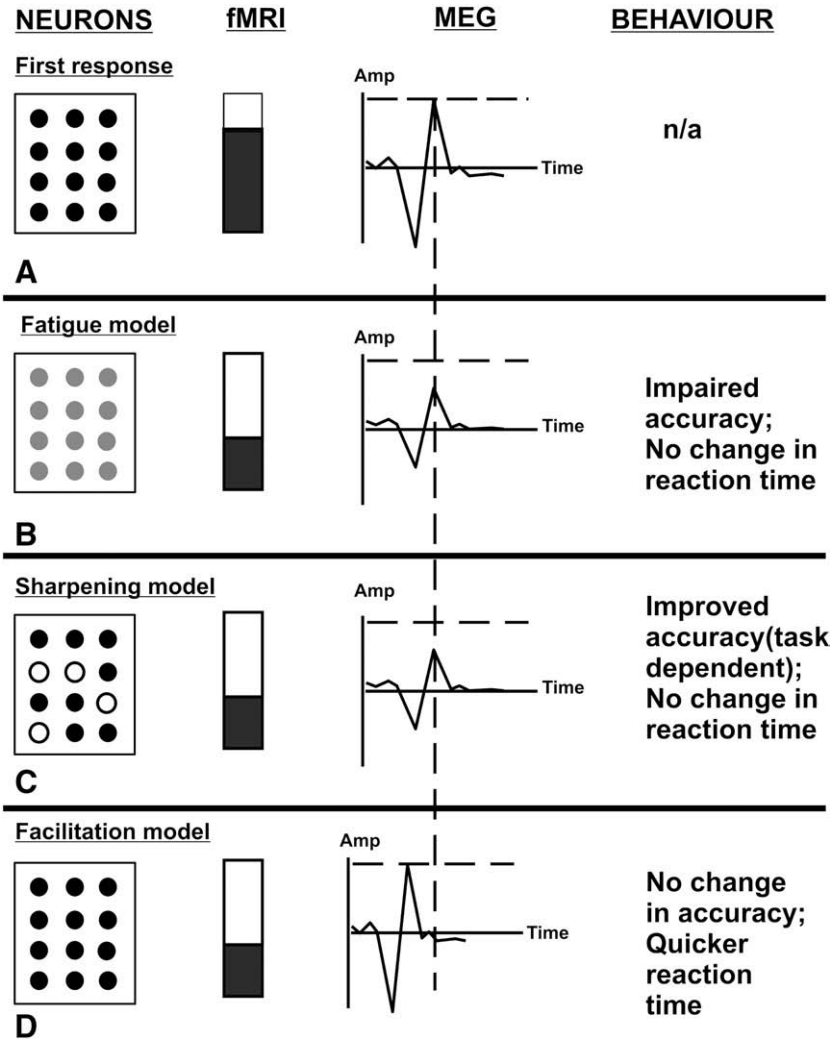

Fig. 1. Diagrammatic representation of the three different models (B–D) with respect to the first response (A) and the predicted effects on the measured signals. The first column represents a population of neurons that are sensitive to the presented stimulus. Row (A) shows the predicted response to the first stimulus. Row (B) refers to the fatigue model and shows an overall reduction in the mean firing rate of all responsive neurons in the population with a predicted reduction in the fMRI, and MEG amplitudes and impairment in the threshold of the behavioural response. Row (C) refers to the sharpening model with only specific neurons responding out of the population causing reduction in the fMRI and MEG responses, but with a possible improvement in the behavioural threshold. Row (D) shows no change in the mean firing rate of the neurons but a timing effect (not shown) is suggested so that neurons respond more quickly. This in turn causes an overall decrease in the fMRI amplitude, a quicker onset of the MEG response and quicker reaction times in the behavioural response.

and suppression will not occur. The choice of ISIs was largely influenced by findings from (Ogawa et al., 2000), that demonstrated conclusively the presence of RS at an ISI of 200 ms in a paradigm design very similar to ours. They found RS to be substantially reduced at 600 ms, thus we chose to include 600 ms as a control to validate any suppression as a RS response.

Methods

Subjects

Approval for this study was obtained from the University of Liverpool Ethics Committee and all volunteers provided signed informed consent prior to their participation. 12 subjects (4 male, 8 female; average age 30 ± 5.5 years) participated in all 3 sessions of the study. All subjects began with the behavioural task first, followed by either a MEG and fMRI (5 subjects) or fMRI and MEG (7 subjects) combination of sessions. Subjects were tested on separate days for each session, and all three sessions were completed within 3 weeks for each individual.

Visual paradigms

RS paradigm

The stimulation paradigm consisted of paired Gabor patches (Fig. 2) in an event-related design. The stimulus was presented to the right of a central fixation cross, in order to activate the left hemisphere of the visual cortex. Each patch was presented for 100 ms and the inter-stimulus interval (ISI) between the two Gabor patches in each pair was set at either 200 ms or 600 ms. The 600 ms condition was chosen as a control based on the finding that no suppression was observed in somatosensory evoked potentials in a similarly designed paradigm in a previous study (Ogawa et al., 2000). The inter-trial interval between pairs of patches was 2 s in both the behavioural and MEG measurements, and was increased to 4 s for the fMRI component to remove any nonlinearities in the BOLD response (Vazquez and Noll, 1998).

In order to create paired conditions termed SAME or DIFF, the first patch was randomised to be either vertical or horizontal in orientation and the second patch was always vertical. Thus, there were 4 conditions, which we refer to as SAME-200, DIFF-200, SAME-600 and DIFF-600, where the number refers to the ISI between the paired patches. The conditions were presented in a random order. A task was introduced to maintain the subjects' attention by a slight modification to the tilt of the second patch. This patch was tilted either to the right or left of the centre by the following angles 0, 0.3, 0.6, 0.9, 1.2, 1.5 degrees. Subjects were required to respond via a button press to indicate the direction the patch was oriented towards. Tilt angles were randomised in all tasks. In house Matlab (Mathworks Inc, USA) routines were used to create the Gabor patches, and stimulation paradigms were created in Presentation (Neurobehavioral Systems Inc., USA). The visual angle subtended to the centre of the patch was 6 degrees, whilst the visual angle diameter was 10 degrees with a spatial frequency of 0.5 cycles/degree. These parameters were maintained in the behavioural, MEG and fMRI tasks. Each subject completed a total of 240 trials of each condition in the MEG experiment, 60 trials of each condition in the fMRI experiment, and, on average 315 ± 52 trials of each condition in the behavioural experiment.

fMRI localiser paradigm

A functional localiser was included in order to independently define the regions of activation produced by the Gabor patches. The stimulus paradigm for the functional localiser scan consisted of alternating horizontal and vertical Gabor patches at 8 Hz in 10 blocks of 10 s interspersed with blocks of rest of the same duration. The location and attributes of the Gabor patches were identical as for the RS paradigm: The visual angle subtended to the centre of the Gabor patch was 6 degrees, the visual angle diameter was 10 degrees and the patches had a spatial frequency of 0.5 cycles/degree.

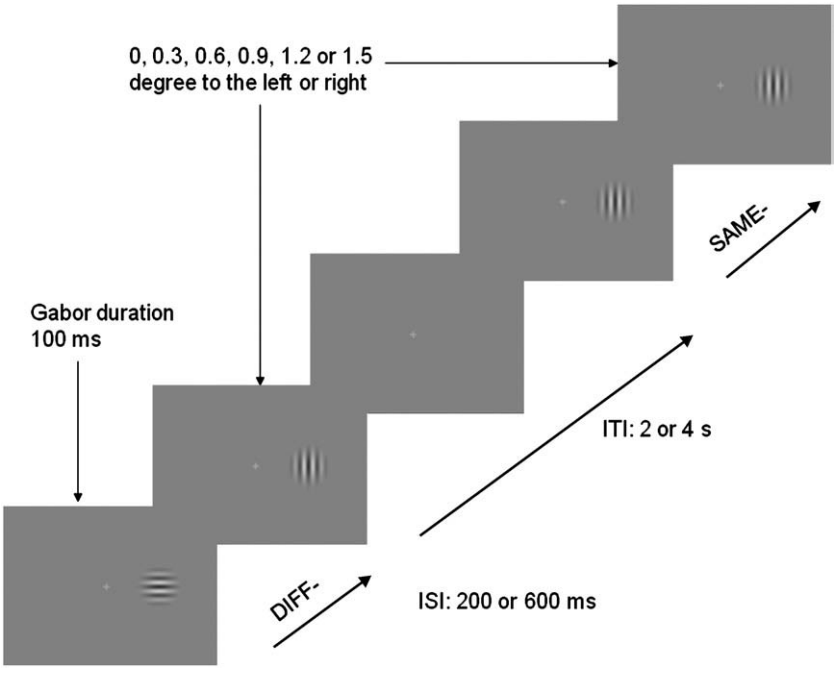

Fig. 2. A segment from the paradigm sequence. The inter-stimulus interval (ISI) refers to the timing difference between each patch in a pair. This was set at either 200 or 600 ms. The timing between a set of paired patches, referred to as the inter-stimulus intervals (ITI) was set for 2 s in the MEG task and behavioural task and 4 s in the fMRI experiment. The first patch was either horizontal or vertical in orientation, whilst the second patch was always vertical, and patches were on for 100 ms each. The pairing of different combinations of vertical–vertical patches (SAME) or vertical–horizontal patches (DIFF) and ISI led to the following four conditions: DIFF-200, SAME-200, DIFF-600 and SAME-600. These were presented in a randomised order. In order to ensure subjects attended to the stimulus, the second patch was tilted slightly by either 0, 0.3, 0.6, 0.9, 1.2 or 1.5 degrees towards the left or the right, and subjects were required to indicate via the use of a button box the direction of tilt.

Retinotopic mapping paradigm

The retinotopic mapping protocol consisted of 2 rotating checkerboard wedges, positioned 180° from one another, rotating for 8 cycles (Slotnick and Yantis, 2003). Each wedge was 25 degrees thick and alternated at 8 Hz with a temporal frequency of 64 s per rotation. In order to ensure subjects attended to the stimulus, a behavioural component was included in this paradigm by the presentation of a red flash in the wedges at random periods. Subjects were required to respond to the presentation of this red flash using a button box.

Data acquisition and analysis

fMRI acquisition

All MRI scans were performed on a Siemens 3 Tesla Trio system using an 8 channel head coil. Each scan session began with an acquisition of a high resolution T_1-weighted structural scan (176 slices; FOV 256 mm × 256 mm, 1 mm isotropic voxels).

This was then followed by 3 runs of the RS paradigm, each consisting of 20 presentations of each of the 4 conditions, along with 20 null events, in a random order (each run of duration 412 s). A standard EPI sequence was used with the following parameters: 38 slices; slice gap = 0.3 mm, TR = 2500 ms, TE = 35 ms, 3 mm isotropic voxels, FOV 192 mm × 192 mm. In keeping with the behavioural and MEG setup, subjects used a button box in the MRI scanner to indicate direction of tilt of the second Gabor patch on each condition.

The localiser task then followed (total duration 200 s), using the same EPI sequence as described above. Finally, the retinotopic mapping run followed (total duration 512 s) which was acquired using a standard EPI sequence with the following parameters: 31 slices; slice gap = 0.3 mm, TR = 2000 ms, TE = 35 ms, 3 mm isotropic voxels, FOV 192 mm × 192 mm.

fMRI analysis

All fMRI data were analysed using BrainVoyager QX (Brain Innovations, Maastricht, The Netherlands, Version 1.10). T_1-weighted structural images were converted to Talairach space. fMRI data was motion corrected and spatial (6 mm full width half maximum (FWHM)) and temporal smoothing (2.8 s FWHM) was applied to subjects' data.

Retinotopic analyses were carried out on an individual basis by first segmenting both grey and white matter in order to define the cortical boundaries. This defined boundary was then inflated to enable easier visualisation of the retinotopic map on a smooth cortical surface. The functional data from the retinotopic run were analysed using a box-car function convolved with the standard hemodynamic response function (HRF) implemented in BrainVoyager (composed of two gamma functions defining the main BOLD response and the post-stimulus undershoot), for a range of 16 lag times (from 0 to 32 s). The lag time represents the visual angle of the stimulus, with 32 s covering one half of the visual field. The significantly activated voxels ($p<0.0005$, Bonferroni corrected) were color-coded for lag time (visual angle) and displayed on the inflated cortical surface. Using knowledge of the retinotopic organization of the visual cortex (Wandell et al., 2005) the visual regions were identified. The localizer data was analysed using a box-car function convolved with the standard HRF and activation was superimposed onto the individual retinotopic maps to determine the visual regions that were activated by the Gabor patch (Fig. 3). Regions of interest (ROI) were identified at threshold of $p<0.05$ (Bonferroni corrected), and then further thresholded so that active clusters were limited to a volume of 0.5 cm^3.

A general linear model was created for the RS runs, including the four paired-patch conditions as regressors. The regressors were convolved with the HRF and fitted to the signal within the ROIs as determined by the functional localiser scan. Beta-weights (relating to

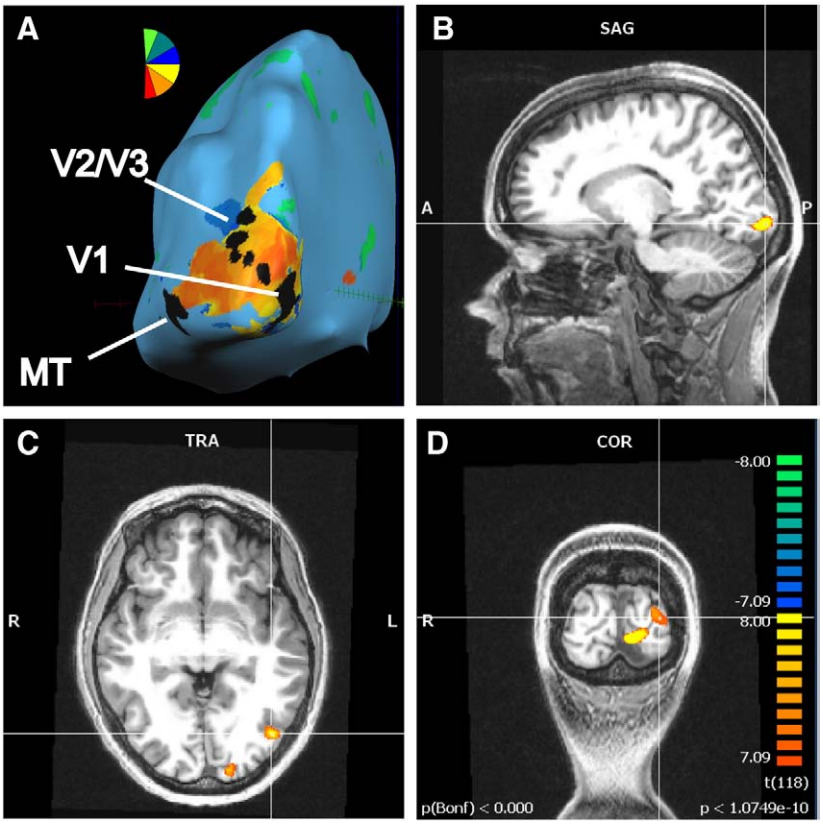

Fig. 3. An example from a single subject showing the response to the functional localiser scan. (A) The localiser activation regions are shown in black, thresholded to $p<0.05$, Bonferroni corrected. In order to identify in which visual areas these reside, they are superimposed onto a retinotopic map (shown as coloured regions representing visual field as shown by the key; thresholded at $p<0.0005$, Bonferroni corrected). These localisation patches are replicated (in yellow) for improved visualisation on the sagittal view for V1 (B), axially for MT (C) and coronally for V2/3 (D).

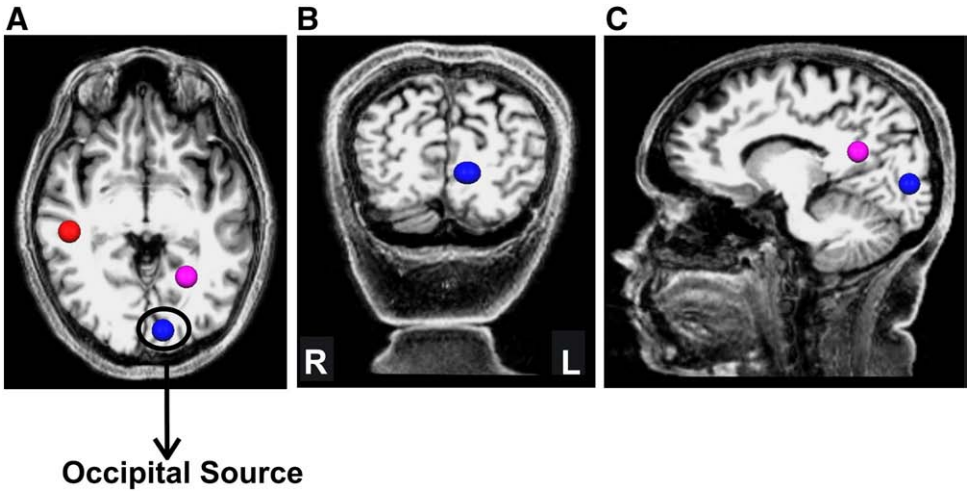

Fig. 4. Sources generated from the response to the first stimulus in a single subject. Five sources were generated (only 3 of these 5 are shown here) using the PCA and Genetic Algorithm in BESA from the first responses in all conditions to improve the localisation of an appropriate occipital source. This occipital source (shown in blue) was used to obtain the evoked responses to the second responses in the different conditions.

the BOLD amplitude) were computed for each condition in each ROI on an individual basis. In order to reduce inter-subject variance the beta-weights were normalised on an individual basis by dividing the signal for each condition by the average signal over all conditions.

MEG acquisition

MEG recordings were performed using a whole-head neuromagnetometer system (4D Neuroimaging WH2500, San Diego, CA, USA), consisting of an array of 148 axial gradiometers encased in a helmet-shaped device, and housed in a magnetically shielded room. Subjects were seated inside the shielded room, and data referencing the orientation, location and shape of the head relative to the MEG sensor was obtained. In particular, coils anchored to the fiducial landmarks on the head (nasion, left and right peri-auricular points) were used to establish a head frame reference system for each subject based on Cartesian coordinates (x, y, z). Furthermore, the location of the subject's head relative to the sensor array was determined using three additional flat coils secured to the forehead. Finally, a tracking device was used to obtain a digital representation of the external head shape, which subsequently was co-registered with the subject's anatomical MRI to increase the localisation accuracy of the evoked electromagnetic activity during source reconstruction. ECG and EOG recordings were acquired simultaneously to aid in artefact removal during post-processing of data. All signals were bandpass-filtered (0–200 Hz) and sampled with 678 Hz frequency.

One subject was excluded from the MEG analysis due to noisy data.

MEG analysis

All post-processing and fitting of data was carried out in BESA (MEGIS Software GmbH). Post-processing of data included removal of ECG and EOG contamination, rejection of bad channels, bandpass filtering of data (2–40 Hz) and averaging data into the relevant epochs of the different conditions. Event related fields were obtained on an individual basis. Responses to each condition were averaged with a zero baseline set between 150 ms and 50 ms before the onset of the first Gabor patch. The sampling window for both ISI's was set so that it began 150 ms before the first Gabor patch and continued for 600 ms for the 200 ISI condition, and 1000 ms for the 600 ISI condition.

In order to find the relevant left occipital dipole, the response to the first flash only, averaged over all conditions, was first modelled in each individual. A Genetic Algorithm (McNay et al., 1996) and a principal component analysis was executed on all individual subjects to account for up to 5 sources (Fig. 4). Identification of occipital sources was chosen based on anatomical location. Most subjects had the 5 sources distributed widely across the brain with a clear source (the blue circle in Fig. 4) in the occipital region. This source was chosen as the occipital source. Individual occipital sources for all subjects are shown in Fig. 5 as confirmation of occipital location. Examination of the Talairach co-ordinates of these sources showed 9 out of the 11 subjects had sources in the occipital cortex. The remaining 2 subjects showed sources close to the occipital cortex, and further investigation of the evoked field responses from these sources displayed evoked field traces similar to that of the other

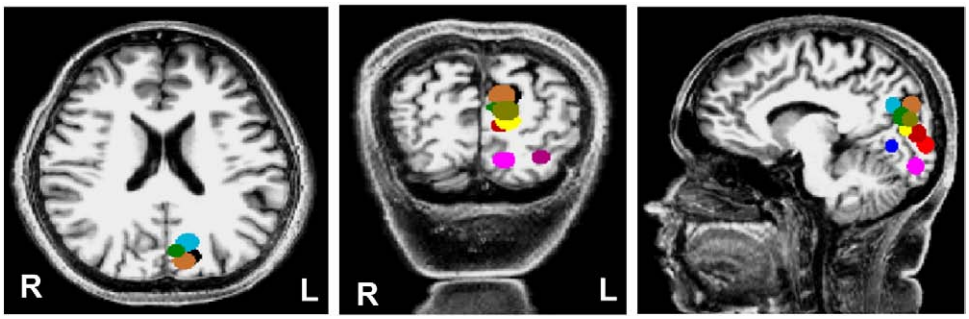

Fig. 5. Individual sources from all 11 subjects (each subject is shown as different coloured circles) that were used to obtain the evoked responses in all conditions shown on a single subject. Each sensor location was obtained using Talairach co-ordinates from individual subjects which were then superimposed onto a single subject's high resolution structural image. Talairach co-ordinates of the planes shown are $x=-10$, $y=-80$, $z=21$.

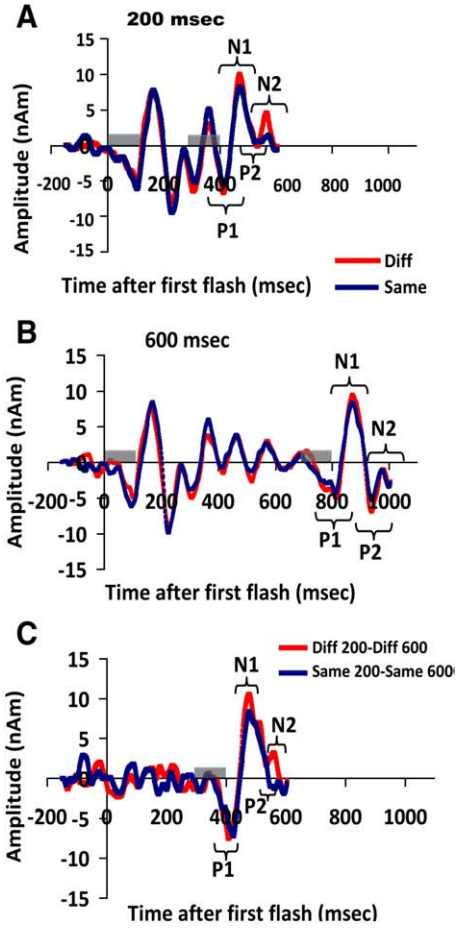

Fig. 6. Averaged evoked field responses from the 11 subjects for the different conditions. Grey blocks represent both the first and second stimulus (flash), and all responses are with respect to the start of the first stimulus. Panel A shows the responses to the 200 ms ISI condition and panel B to the 600 ms ISI conditions for the SAME and DIFF conditions. Panel C shows the response to the second Gabor patch only following the subtraction of the first response (thus there is no grey bar indicating the presence of the first stimulus). This subtraction was to reduce contributory effects (to the analysis) that may be derived from ongoing oscillatory activity from the response to the first Gabor patch. Paired *t*-tests on the peaks of the second responses of the two conditions revealed a significant reduction ($p<0.05$) in the SAME- 200 condition compared to that of the DIFF- 200 condition in the final peak.

visual sources. The other 4 sources included as part of the algorithm were not present in consistent locations across subjects and therefore were not included in the analysis. The solution of the dipole from the left occipital area was then used to acquire the evoked responses from all 4 conditions. These source dipole waveforms were averaged over all subjects to obtain the averaged traces for all conditions (Figs. 6A, B). The peak amplitude of the 4 peaks (labelled N1, P1, N2, P2 in Fig. 6), following the onset of the second flash, and the corresponding latencies were obtained from individual traces, and

Table 1a
Peak latencies.

Peak	DIFF-200	SAME-200	DIFF-600	SAME-600
P1	94 ± 48	89 ± 41	102 ± 22	91 ± 23
N1	161 ± 39	148 ± 28	179 ± 44	153 ± 25
P2	214 ± 39	213 ± 43	229 ± 30	223 ± 42
N2	268 ± 22	262 ± 32	280 ± 29	271 ± 31

Peak latencies (ms) from the major 4 peaks of the second response (as shown in Fig. 6a and b), with respect to the onset of the second stimulus. Mean ± SD are shown across 11 subjects. No significant differences between peak latencies of the SAME and DIFF conditions were found.

Table 1b
Peak amplitudes.

Peak	DIFF-200	SAME-200	DIFF-600	SAME-600
P1	−10.4 ± 7.4	−9.2 ± 5.2	−11.1 ± 5.9	−10.6 ± 5.2
N1	13.9 ± 9.9	11.0 ± 9.0	15.2 ± 10.0	12.8 ± 8.4
		**		*
P2	−7.0 ± 7.9	−7.7 ± 6.0	−5.4 ± 14.6	−10.6 ± 5.1
N2	8.7 ± 9.2	5.7 ± 8.1	2.4 ± 7.5	2.9 ± 8.3
		*		

Mean peak amplitudes (nAm) from the major 4 peaks of the second response (as shown in Figs. 6A and B) averaged across all 11 subjects. Mean ± SD are shown. *t*-tests revealed significant reduction of the SAME amplitudes in comparison to DIFF, where ** denotes $p<0.01$ and* denotes $p<0.05$.

two tailed paired Student *t*-tests were carried out on these data sets to test differences in peak amplitudes and latencies between conditions (Table 1a and b). In order to remove contamination from the response to the first flash in the 200-ms ISI condition, the 600 -ms ISI condition waveform (up to 600 ms post-stimulus onset, when only the response to the first flash is present) was subtracted from the 200 -ms ISI condition waveform on an individual basis and then averaged (Fig. 6C). SAME-600 conditions were subtracted from SAME-200 conditions and DIFF-600 from DIFF-200. This approach assumes that, following presentation of the second Gabor patch, the overall MEG response to the 200 ms condition is a linear sum of the response to the individual Gabor patches. This subtraction approach is common in EEG studies (Thorpe et al., 1996) and there is supporting evidence that MEG responses do add linearly on such timescales (Supek et al., 1999).

Behavioural data analysis

In-house Matlab routines were used to obtain percent correct responses from each subject for all tilt angles and reaction times to averaged conditions. The percentage correct response as a function of tilt angle was fitted to a Weibull function and the 75% correct point was extracted as the threshold of the tilt detection for each condition and each subject.

Results

Behavioural data

One subject was excluded from the final data analysis due to poor performance of the task; i.e. the 75% threshold was above the range of angles tested for all 4 conditions. Fig. 7 shows the behavioural performance averaged over 11 subjects. It can be seen that the response accuracy with regard to subjects' ability to judge the direction of the tilt showed a significant impairment (two-tailed paired *t*-test, $p<0.05$) at the SAME-200 condition (Fig. 7A) compared to all other conditions. One may have expected an improved ability to gauge the direction of tilt of the second patch when it is preceded by another vertical patch (thus providing a "true" reference of vertical), however an impairment is seen when compared to the DIFF-200 condition. This impairment is only seen at an ISI of 200 ms, with thresholds recovering to the same level as for the DIFF- condition at ISI of 600 ms (Fig. 7B). Hence, there is an orientation-driven effect in performance accuracy at 200 ms ISI only. Mean response times were also obtained for the different conditions across 11 subjects. The response times for the DIFF- conditions (312 and 302 ms for 200 and 600 ms ISI, respectively) were significantly quicker than for the SAME-conditions (381 and 375 ms for 200 and 600 ms ISI, respectively). Two-tailed paired *t*-tests confirmed the DIFF- response time to be significantly quicker at both 200 ms ISI ($p<0.0001$) and 600 ms ISI ($p<0.00001$). In contrast to the performance accuracy there appears to be an orientation-driven effect in response time at both 200 ms and 600 ms ISI.

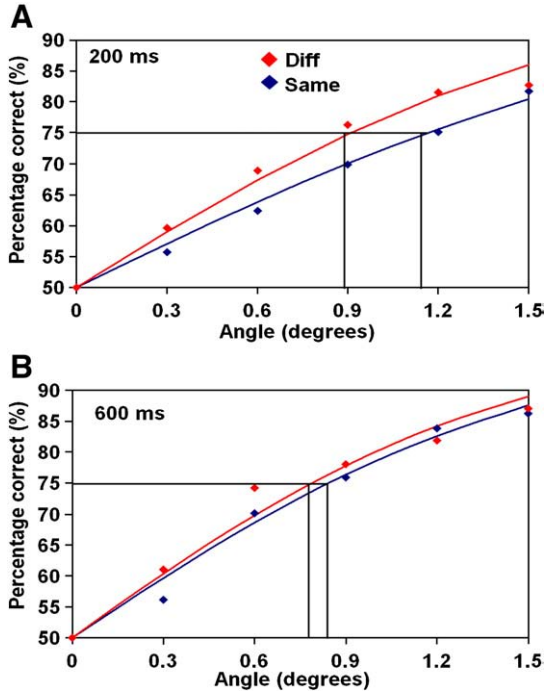

Fig. 7. Behavioural results showing the percentage of correct responses for each tilt angle averaged over all subjects. The Weibull function fit to the average data is shown. Panel A shows that the SAME-200 condition gives a higher detection threshold (1.14 degrees) compared to the DIFF-200 condition (0.88 degrees). A two-tailed paired *t*-test across subjects confirmed that this was significant at $p=0.03$. Panel B shows that at 600 ms ISI, this difference is no longer apparent ($p=0.2$). The SAME-200 thresholds were also found to be significantly higher than both of the 600 ms ISI conditions (SAME-600: 0.81 degrees; DIFF-200: 0.77 degrees). Error bars represent the standard error across subjects.

fMRI Data

The functional localiser showed 4 distinct areas of activation, V1, V2/V3 in both the ventral and dorsal pathways, and MT (Fig. 3) that were consistently activated in the majority of subjects. All 12 subjects showed activation in V1, 8 showed activation in V2/3 and 8 showed activation in MT. A small number of subjects also showed activation in V3a (3 subjects) and V4 (2 subjects), although, due to the poor quality of the retinotopic maps, it was often difficult to accurately distinguish these regions from V2/V3. Due to the position of the stimulus on the horizontal meridian, activation in V2 and V3 was merged and hence it was not possible to separate the activation into these two separate regions. The ventral and dorsal V2/V3 regions were combined, and thus three regions, where the majority of subjects showed activation (V1, V2/V3, and MT), were used as ROI's to obtain beta-weights of the BOLD responses for the RS runs.

Fig. 8 shows the normalised beta-weights, averaged across all subjects in the three ROIs with regards to the RS runs. The BOLD response to the SAME- condition was significantly (paired two tailed *t*-test, $p<0.05$) reduced compared to the DIFF- condition at 200 ms ISI in all three visual areas.

Importantly, paired *t*-tests showed no significant (paired, two tailed *t*-test, $p=0.6$, 0.9 and 0.4 for V1, V2/3 and MT, respectively) differences in BOLD responses between the DIFF- and SAME-conditions at 600 ms, which suggests no orientation effect at this ISI. This supports findings from previous literature that set the ISI of 600 ms as an appropriate temporal control (Ogawa et al., 2000) at which RS is not observed.

MEG data

The MEG evoked fields averaged across all subjects for all four conditions are shown in Fig. 6 (A) and (B). Individual peak amplitudes and their correlating latencies were obtained for the different conditions following the onset of the second flash (Tables 1a and b). From the averaged values (Table 1b) it can be seen that the SAME-200 condition shows a suppression (relative to the DIFF-200 condition) that is significant at N1 with latency of approximately 155 ms (paired, two-tailed *t*-test $p<0.01$) and N2 with latency of approximately 265 ms (paired, two-tailed *t*-test $p<0.03$) following the 2nd stimulus. None of the conditions showed a significant ($p>0.05$) difference in latency (Table 1a). An additional finding was a smaller but nevertheless significant difference at the 600 ms ISI for N1 at latency of approximately 165 ms between the SAME and DIFF conditions (paired, two-tailed *t*-test, $p<0.05$). There was concern that not all MEG dipole sources were located within the occipital cortex (Fig. 5). Therefore, the analysis was repeated using only data from the 9 subjects with occipital dipoles. This revealed a similar trend in reduced N1 and N2 peaks for the SAME-200 condition compared to the DIFF-200 condition with statistical significance for N1 altering to $p<0.05$ and N2 to $p=0.06$, potentially due to the change in statistical power.

It is apparent from Fig. 6A that there is ongoing oscillatory activity following the first stimulus which, for the 200 ms ISI, is clearly overlapping with the response to the second stimulus. It was important to clarify whether this oscillatory activity contributed to the observed suppression and which of these effects were related to repetition suppression. In order to remove the effect of this induced oscillatory activity from the response to the second stimulus in the 200 ms ISI conditions, a subtraction was carried out where the response to the first stimulus alone, as is better characterised by the 600 ms ISI condition, is subtracted from the 200 -ms ISI condition. The resulting average curves for these leave only the second responses for the 200 -ms ISI as shown in Fig. 6C. Statistical analyses of the outstanding peaks from the second response alone showed that there was a significant suppression (paired, two-tailed *t*-test, $p<0.05$) of the last peak of the SAME-condition compared to the DIFF- condition (peak N2 of Fig. 6A), at about 260 ms after the onset of the second stimulus, whilst the previously observed significant suppression observed at N1 disappeared. These findings suggest that the difference seen in N2 of Fig. 6A is due to repetition suppression.

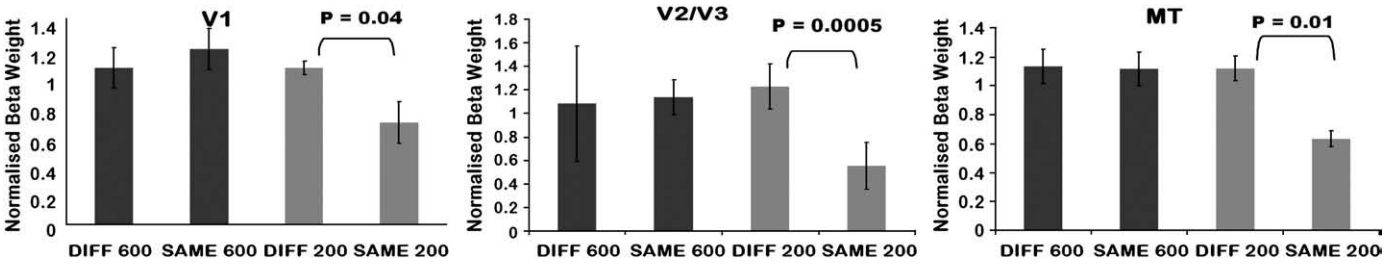

Fig. 8. Normalised BOLD beta-weights for each condition in each visual area averaged across subjects, ($n=12$ for V1, $n=8$ for V2/V3 and $n=8$ for MT). All areas showed a reduction in BOLD amplitude in the SAME-200 condition relative to the other condition. Paired two-tailed *t*-tests show the reduction is significant when compared to the DIFF-200 condition. The error bars represent the standard error across subjects.

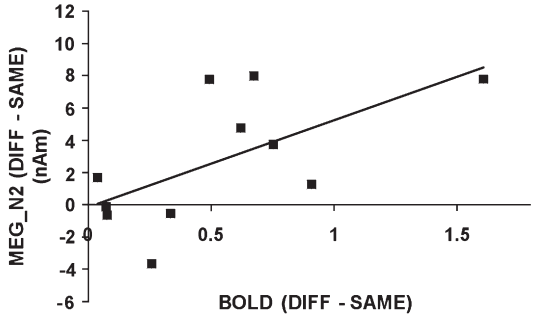

Fig. 9. Correlation plot of amplitude differences (DIFF–SAME) from peak N2 (MEG) and BOLD amplitude differences from the entire visual cortex in the 200 ms ISI for individuals. Significant correlation shown ($r^2 = 0.39$, $p < 0.04$).

In order to relate the MEG and BOLD data, a correlation analysis between the MEG amplitude reduction of peak N2, showing the largest RS effect and the reduction in the BOLD response in the entire visual cortex was carried out. The difference between the SAME and DIFF amplitudes in both the MEG and the BOLD data was compared for the 200 ms ISI condition. A positive correlation (linear regression, $r^2 = 0.39$, $p < 0.04$, Fig. 9) was derived for this relationship, and this correlation was still significant ($p < 0.05$) following the removal of the outlying data point, suggesting that RS observed from these two modalities originate from the same neuronal source.

Discussion

This study addressed the neuronal phenomenon of repetition suppression in the visual cortex using a multimodal approach. The key aim was to consolidate data from these different modalities, using the same experimental paradigm, and to explain the findings with a specific model of RS as proposed previously (Grill-Spector et al., 2006).

RS within different visual areas

Incorporating a retinotopic map, we aimed to establish the level of RS present in the different visual areas. fMRI data showed evidence of RS in all visual areas studied: V1, V2/V3, and MT. Previous studies have not found orientation-specific adaptation in V1 for such brief periods of adaptation (Boynton and Finney, 2003), however Fang et al. (2005) does report suppression in V1 for long (20 s) adaptation duration. Boynton and Finney (2003) showed no RS in V1, however, the shortest inter-stimulus interval that Boynton and Finney (2003) considered was 1.125 s, and the results are therefore in broad agreement with our findings as the suppression we see at 200 ms ISI is no longer present at 600 ms ISI. The study by Murray et al. (2006) used similar adaptation times (200 ms compared to 100 ms used in our study) and the same ISI (200 ms) but did not find evidence for RS in V1. This could be attributable to the different spatial properties of their stimuli, using a dense array of smaller Gabor patches at higher spatial frequency. In addition, none of these previous studies used an orientation-specific task. It may be that attention to the orientation of the stimulus is required to find this orientation-specific RS effects in V1. In general, if adaptation of fMRI-BOLD response is sensitive to neuronal properties, then orientation-specific suppression would be expected in V1 as V1 clearly contains orientation-sensitive cells (Hubel and Wiesel, 1968; Tootell et al., 1998).

In accordance with other studies (Fang et al., 2005; Murray et al., 2006), we found RS to be present in V2/V3, however we also found RS present in MT, an area thought to be involved in the processing of moving visual stimuli (Tootell et al., 1995; Wandell et al., 2005) rather than orientation. However, orientation sensitive neurons have been reported in MT (Albright, 1984), which could explain our findings. Larsson et al. (2006) also reported the presence of orientation sensitive neurons in several visual areas, including MT, using fMR-adaptation paradigms in human brains. Alternatively, RS in MT may be due to the feed-forward signal from the V1 cells (Kohn and Movshon, 2004), i.e. if signal is reduced in V1 then it may also be reduced in MT.

Another possible explanation could be that the "DIFF-" and "SAME-stimuli" appeared to have different motion characteristics, that is, apparent motion is seen for the DIFF- case, which may lead to an increase in attention and consequently a larger signal for the DIFF 200 case. Based on approximate speed of the apparent motion, both the 200 ms and 600 ms ISI conditions would be expected to cause an apparent motion effect in both V1 and MT (Priebe et al., 2006). Hence if apparent motion was a significant factor leading to the observed suppression, it would have perhaps been seen at both ISI's, which is not the case. It is however difficult to unequivocally rule out the role of apparent motion as there are factors present in Priebe et al. (2006) work that is not directly comparable to the current study.

Additionally, behavioural data (not reported) showed that subjects had a high response rate (98%) to the stimuli for all conditions at both ISI's with no significant difference between SAME and DIFF, thus suggesting high attention in all conditions. Reaction times were quicker for the DIFF stimuli at both 200 and 600 ms ISI, thus suggesting that any attention related difference is not the cause of the observed suppression.

In this study the paradigm design was limited to an initial presentation of a vertical or horizontal patch and the subsequent presentation of a vertical patch in all trials. This potentially lends an extra variable to the paradigm design. Past studies have observed differences in the level of activation to vertical and horizontal stimuli, present in V1 of the cat striate cortex using multi unit recordings (Li et al., 2003) and the human cortex using fMRI (Furmanski and Engel, 2000). However, the temporal resolution of MEG allows us to separate the response from the two repeated stimuli, and so compare the second response (to vertical stimulus alone) independently across conditions. Assuming linearity of the signal, the effects of the first stimulus can be completely subtracted from the second response (Fig. 6C), thus isolating the true repetition suppression effect. It is not possible to separate the response to the two stimuli in the fMRI data. However, on the basis of the papers by Li et al. (2003) and Furmanski et al. (2000), the effect of any difference in fMRI response to horizontal and vertical stimuli is small and is restricted to V1, and cannot account for the large reductions seen in all visual areas (approximately 40%, Fig. 8). Eye movements were not recorded in this study, which in hindsight would have been a useful measure. It can be argued however that since adaptation was observed, eye movement must have been minimal, as any eye movements would have destroyed any adaptation effect due to the small receptive field size in V1.

We find RS in areas not traditionally believed to be involved in orientation processing, hence perhaps an important finding from the fMRI data is that care should be practiced when interpreting data from studies reporting on adaptation of fMRI-BOLD responses to repeated stimuli, especially since it is widely used as a tool to interpret the role of brain areas in the processing of specific stimuli.

The importance of adaptation duration

Fang et al. (2005) argue that the absence of V1 activation in the study of Boynton and Finney (2003) could be accounted for by the duration of adaptation. They suggest a strong temporal component to the observation of RS in V1, such that adaptation times lasting tens of seconds lead to a measurable RS and adaptation times of 1 s and less showed no RS. However our study shows clear RS in V1 with an adaptation time of only 100 ms. In support, single electrode measurements Muller et al. (1999) have shown RS with adaptation duration of 500 ms, with complete recovery of the cell's sensitivity

during the 2-s rest period. Additionally, Kourtzi and Kanwisher (2001) showed RS in a paradigm employing an adapting stimulus with a duration of 300 ms in an fMRI study. The differences abiding to the measurement of RS at different time scales hints that there may be different underlying neurophysiological processes sensitive to the adaptation duration of the stimulus. The choice of an appropriate inter-stimulus interval is also pivotal in the observation of RS. Our choice of ISI's at 200 ms and 600 ms was largely influenced by work carried out by Ogawa et al. (2000). Their study incorporating somatosensory evoked potentials and BOLD measurements in the rat model across a series of ISIs showed the largest RS at 200 ms ISI and reduced RS at 600 ms ISI. Interestingly, both our MEG and BOLD data was in agreement with this study, and furthermore, our behavioural study also showed a strong dependency on the ISI with subjects demonstrating impaired performance at 200 but not 600 ms ISI. This dependency would suggest that the choice of ISI is pivotal, especially to reduce the possibility of mis-interpretation of a null result.

RS measured by MEG

In contrast to the fMRI data, MEG data did not show such a large RS effect. However, for the 200 ms ISI condition, RS was observed at both 155 ms and 265 ms after the second stimulus onset (Fig. 6A). This is in accordance with Henson et al. (2004) that show RS between 160–190 ms and 200-300 ms in EEG measurements responding to visual stimuli. Although smaller than for the 200 ISI condition, RS was also observed in the 600 ISI condition at 165 ms, which was not replicated in the fMRI. This observation suggests that RS is still present at an ISI of 600 ms, and is perhaps not seen in the fMRI due to temporal averaging of the BOLD signal over the complete stimulus. Statistical analysis on the latencies of the onset of the MEG peaks, showed no significant differences between the different conditions, which is in direct contradiction with another study (Noguchi et al., 2004) that used MEG to observe the presence of RS in the visual ventral stream who found a decrease in the onset of the suppressed response peak. This difference may be attributed to their paradigm design which incorporated moving dots. Motion driven stimulus has been shown to have an effect on the response latencies due to the different processing stream involved for motion stimuli as opposed to shape stimuli (Schoenfeld et al., 2003).

Behavioural effects of stimulus repetition

We report a consistent behavioural effect, with impairment of orientation discrimination for the SAME-200 condition compared to all other conditions. This matches the fMRI and MEG results where an RS effect was seen for the SAME-200 condition, suggesting that the underlying neural mechanism is shared. The effect of adaptation on orientation discrimination is well documented as the "tilt after effect," where the test stimulus appears repelled away from the adapter for small adapting orientations, causing improvements in orientation discrimination (Clifford, 2002). We observe however an impairment of discrimination following adaptation around vertical. This discrepancy could be due to the very short adapting duration (100 ms). Indeed, previous work using briefer adapting stimuli (400 ms) supports our findings, confirming that orientation discrimination is impaired after iso-orientation adaptation (Dragoi et al., 2000).

Relating BOLD, MEG and behavioural measures of RS

One aim of this study was to consider how the combination of fMRI, MEG and behavioural data support the fatigue, sharpening or facilitation models. In Fig. 1 we form predictions relating to the responses from the three different measuring modalities according to the models.

The facilitation model is best modelled by a recurrent neural network (Becker et al., 1997) by which strengthened connections within co-active nodes lead to reduced processing time of the repeated stimulus. This would produce earlier peaks in the MEG signal and quicker reaction times for the behavioural responses for the SAME condition, neither of which were observed.

In contrast, the sharpening model suggests that only specific neurons, those most tuned to the repeated feature, respond to the second repeated stimuli, thus there is an overall reduction in the number of neurons responding. In MEG and fMRI this would lead to a reduced response, as fewer neurons contribute to the measured signal. Support for the sharpening model has emerged primarily from single electrode measurements (Brown et al., 1987; Wiggs and Martin, 1998) carried out in animal models. The fMRI and MEG data both show a reduction in response to the second stimulus, thus supporting the sharpening model. The behavioural data show impaired ability to discriminate angles around vertical, which would not immediately be expected if the responding neurons are those most tuned to vertical. However, there is evidence that discrimination is most effective for angles on the flanks of the tuning curve (Scobey and Gabor, 1989), and hence that neurons tuned away from vertical may be most able to discriminate around vertical. Hence, a sharpening mechanism could be responsible for the impairment seen in behaviour.

The fatigue model describes an overall reduction in the firing rate of all neurons to the repeated stimulus. In a tightly coupled system, this reduction in firing rate would in turn lead to a local reduction in the neurotransmitter release which would cause a reduction in the BOLD signal (Attwell and Iadecola, 2002). Hence this model would predict a reduction in both MEG and BOLD which is seen in our data. A reduction in firing rate in neurons tuned to the adapting stimulus, as seen in the work by Muller et al. (1999), could cause a shift in population tuning away from the adapting stimulus (Dragoi et al., 2002). This would lead to an impairment in orientation discrimination for the SAME stimulus, which is confirmed by our behaviour data. Hence our measurements also provide support for the fatigue model for the current paradigm.

An electrophysiological study conducted by Sawamura et al. (2006) looked at the response of a population of neurons that were tuned at varying degrees to specific visual stimuli. It was shown that the degree of adaptation was not closely related to how optimally tuned the neuron was to the stimulus. It is our belief that these data reduce the applicability of the sharpening model as an appropriate model of RS. It is important to acknowledge the possibility that the fatigue, sharpening and facilitation models may all be valid models of RS depending on the paradigm design, and our conclusion reflects the behaviour of the neuronal population implicated in the current paradigm.

In summary, in all three modalities we find an effect of repetition for the 200 ms ISI condition. This is seen as a suppression of the BOLD response in all the visual areas we examined, a reduction of the MEG response at 155 and 265 ms after the second stimulus and impairment in orientation discrimination. This correspondence of the data from MEG, fMRI and behaviour shows quite clearly that RS is a neuronal phenomenon, and not just a vascular phenomenon as is postulated in previous studies (Murray et al., 2006). The degree of suppression measured with MEG and with the BOLD response is correlated over subjects thus indicating that these signals are derived from the same source. The relation between MEG, BOLD and behaviour shown in this study confirms the neural source of the fMR-adaptation response, and provides further information regarding the underlying mechanism. In the current paradigm, we present evidence against the facilitation model, but cannot distinguish between the sharpening or fatigue models.

Acknowledgments

This study was supported by the Medical Research Council (MRC) UK. We wish to thank Dr. Roozbeh Rezaie for his support with the MEG measurements.

References

Albright, T.D., 1984. Direction and orientation selectivity of neurons in visual area MT of the macaque. J. Neurophysiol. 52, 1106–1130.
Attwell, D., Iadecola, C., 2002. The neural basis of functional brain imaging signals. Trends Neurosci. 25, 621–625.
Becker, S., Moscovitch, M., Behrmann, M., Joordens, S., 1997. Long-term semantic priming: A computational account and empirical evidence. J. Exp. Psyc Learn. Mem. Cog. 23, 1059–1082.
Bonhoeffer, T., Grinvald, A., 1991. Iso-orientation domains in cat visual cortex are arranged in pinwheel-like patterns. Nature 353, 429–431.
Boynton, G.M., Finney, E.M., 2003. Orientation-specific adaptation in human visual cortex. J. Neurosci. 23, 8781–8787.
Brown, M.W., Wilson, F.A.W., Riches, I.P., 1987. Neuronal evidence that inferomedial temporal cortex is more important than hippocampus in certain processes underlying recognition memory. Brain Res. 409, 158–162.
Clifford, C.W.G., 2002. Perceptual adaptation: motion parallels orientation. Trends Cog. Sci. 6, 136–143.
Dragoi, V., Sharma, J., Miller, E.K., Sur, M., 2002. Dynamics of neuronal sensitivity in visual cortex and local feature discrimination. Nat. Neurosci. 5, 883–891.
Dragoi, V., Sharma, J., Sur, M., 2000. Adaptation Induced Plasticity of Orientation Tuning in Adult Visual Cortex. Neuron 28, 287–298.
Fang, F., Murray, S.O., Kersten, D., He, S., 2005. Orientation-tuned fMRI adaptation in human visual cortex. J. Neurophysiol. 94, 4188–4195.
Furmanski, C.S., Engel, S.A., 2000. An oblique effect in human primary visual cortex. Nat. Neurosci. 3, 535–536.
Grill-Spector, K., Henson, R., Martin, A., 2006. Repetition and the brain: neural models of stimulus-specific effects. Trends Cog. Sci. 10, 14–23.
Grill-Spector, K., Kushnir, T., Edelman, S., Avidan, G., Itzchak, Y., Malach, R., 1999. Differential processing of objects under various viewing conditions in the human lateral occipital complex. Neuron 24, 187–203.
Henson, R.N.A., 2003. Neuroimaging studies of priming. Prog. Neurobiol. 70, 53–81.
Henson, R.N.A., Rugg, M.D., 2003. Neural response suppression, haemodynamic repetition effects, and behavioural priming. Neuropsychologia 41, 263–270.
Henson, R.N., Rylands, A., Ross, E., Vuilleumeir, P., Rugg, M.D., 2004. The effect of repetition lag on electrophysiological and haemodynamic correlates of visual object priming. Neuroimage 21, 1674–1689.
Hubel, D.H., Wiesel, T.N., 1968. Receptive fields and functional architecture of monkey striate cortex. J. Phys. Lond. 195, 215–243.
James, T.W., Gauthier, I., 2006. Repetition-induced changes in BOLD response reflect accumulation of neural activity. Hum. Brain Mapp. 27, 37–46.
Kohn, A., Movshon, J.A., 2004. Adaptation changes the direction tuning of macaque MT neurons. Nat. Neurosci. 7, 764–772.
Kourtzi, Z., Kanwisher, N., 2001. Representation of perceived object shape by the human lateral occipital complex. Science 293, 1506–1509.
Li, B.W., Peterson, M.R., Freeman, R.D., 2003. Oblique effect: a neural basis in the visual cortex. J. Neurophysiol. 90, 204–217.
McNay, D., MichielssenIssen, E., Rogers, R.L., Taylor, S.A., Akhtari, M., Sutherling, W.W., 1996. Multiple source localization using genetic algorithms. J. Neurosci. Methods 64, 163–172.
Movshon, J.A., Lennie, P., 1979. Pattern selective adaptation in visual corticol neurones. Nature 278, 850–852.
Muller, J.R., Metha, A.B., Krauskopf, J., Lennie, P., 1999. Rapid adaptation in visual cortex to the structure of images. Science 285, 1405–1408.
Murray, S.O., Wojciulik, E., 2004. Attention increases neural selectivity in the human lateral occipital complex. Nat. Neurosci. 7, 70–74.
Murray, S.O., Olman, C.A., Kersten, D., 2006. Spatially specific fMRI repetition effects in human visual cortex. J. Neurophysiol. 95, 2439–2445.
Noguchi, Y., Inui, K., Kakigi, R., 2004. Temporal dynamics of neural adaptation effect in the human visual ventral stream. J. Neurosci. 24, 6283–6290.
Ogawa, S., Lee, T.M., Stepnoski, R., Chen, W., Zhuo, X.H., Ugurbil, K., 2000. An approach to probe some neural systems interaction by functional MRI at neural time scale down to milliseconds. Proc. Natl. Acad. Sci. U. S. A. 97, 11026–11031.
Priebe, N.J., Lisberger, S.G., Movshon, J.A., 2006. Tuning for spatiotemporal frequency and speed in directionally selective neurons of macaque striate cortex. J. Neurosci. 26, 2941–2950.
Sawamura, H., Georgieva, S., Vogels, R., Vanduffel, W., Orban, G.A., 2005. Using functional magnetic resonance imaging to assess adaptation and size invariance of shape processing by humans and monkeys. J. Neurosci. 25, 4294–4306.
Sawamura, H., Orban, G.A., Vogels, R., 2006. Selectivity of neuronal adaptation does not match response selectivity: a single-cell study of the fMRI adaptation paradigm. Neuron 49, 307–318.
Schoenfeld, M.A., Woldorff, M., Duzel, E., Scheich, H., Heinze, H.J., Mangun, G.R., 2003. Form-from-motion: MEG evidence for time course and processing sequence. J. Cogn. Neurosci. 15, 157–172.
Scobey, R.P., Gabor, A.J., 1989. Orientation discrimination sensitivity of single units in cat primary visual cortex. Exp. Brain Res. 77, 398–406.
Slotnick, S.D., Yantis, S., 2003. Efficient acquisition of human retinotopic maps. Hum. Brain Mapp. 18, 22–29.
Supek, S., Aine, C.J., Ranken, D., Best, E., Flynn, E.R., Wood, C.C., 1999. Single vs. paired visual stimulation: superposition of early neuromagnetic responses and retinotopy in extrastriate cortex in humans. Brain Res. 830, 43–55.
Thorpe, S., Fize, D., Marlot, C., 1996. Speed of processing in the human visual system. Nature 381, 520–522.
Tootell, R.B.H., Reppas, J.B., Kwong, K.K., Malach, R., Born, R.T., Brady, T.J., Rosen, B.R., Belliveau, J.W., 1995. Functional-analysis of human MT and related visual cortical areas using magnetic resonance imaging. J. Neurosci. 15, 3215–3230.
Tootell, R.B.H., Hadjikhani, N.K., Vanduffel, W., Liu, A.K., Mendola, J.D., Sereno, M.I., Dale, A.M., 1998. Functional analysis of primary visual cortex (V1) in humans. Proc. Natl. Acad. Sci. U. S. A. 95, 811–817.
Vazquez, A.L., Noll, D.C., 1998. Nonlinear aspects of the BOLD response in functional MRI. Neuroimage 7, 108–118.
Vuilleumier, P., Henson, R.N., Driver, J., Dolan, R.J., 2002. Multiple levels of visual object constancy revealed by event-related fMRI of repetition priming. Nat. Neurosci. 5, 491–499.
Wandell, B.A., Brewer, A.A., Dougherty, R.F., 2005. Visual field map clusters in human cortex. Phil. Trans. R. Soc. B 360, 693–707.
Wiggs, C.L., Martin, A., 1998. Properties and mechanisms of perceptual priming. Curr. Opin. Neurobiol. 8, 227–233.